Available online at www.sciencedirect.com
SCIENCE DIRECT
Journal of Power Sources 157 (2006) 709–713
JOURNAL OF POWER SOURCES
www.elsevier.com/locate/jpowsour

Short communication

Sol–gel derived $(La_{0.8}M_{0.2})CrO_3$ (M=Ca, Sr) coating layer on stainless-steel substrate for use as a separator in intermediate-temperature solid oxide fuel cell

E. A Lee [a], S. Lee [a], H.J. Hwang [a,*], J.-W. Moon [b]

[a] *School of Materials Science and Engineering, Inha University, Incheon, Korea*
[b] *Korea Institute of Ceramic Engineering and Technology, Seoul, Korea*

Received 1 October 2005; accepted 9 December 2005
Available online 7 February 2006

Abstract

A ceramic coating technique is applied to reduce the voltage drop caused by oxidation of the metallic separator (SUS444) in intermediate-temperature (IT) solid oxide fuel cell (SOFCs) systems. Precursor solutions for (La, Ca)CrO_3 (LCC) and (La, Sr)CrO_3 (LSC) coatings are prepared by adding nitric acid and ethylene glycol into an aqueous solution of lanthanum, strontium (or calcium) and chromium nitrates. Dried LCC and LSC gel films are heat-treated at 400–800 °C after dip-coating on the SUS444 substrate. XRD and Fourier-transform infrared (FT-IR) analysis is used to examine the crystallization behaviour and chemical structure of the precursor solution. The oxidation behaviour of the coated SUS444 substrate is compared with an uncoated SUS444 substrate. The oxidation of the SUS444 is inhibited by the LCC and LSC thin film layers.

Keywords: Solid oxide fuel cells; Separator; Sol–gel; Oxidation; Chemical structure

1. Introduction

Compared with other generator systems, fuel cells show high energy efficiency because they can directly convert chemical energy to electrical energy. Furthermore, they emit less pollutants and thus offer environmental advantages [1]. Solid oxide fuel cells (SOFCs) usually operate at high temperatures, and this results in several advantages such as hybridization with a turbine engine, spontaneous reforming inside the system and flexibility in the choice of fuel [2]. On the other hand, their high operating temperature (800–1000 °C) causes both physical and chemical degradation of the construction materials and limits the choice of materials that can be used for their fabrication. In addition, the high operating temperature requires lanthanum chromite-based ceramic separators to be used that are very expensive and difficult to fabricate and machine.

Separator materials have to satisfy some requirements namely (i) they must be chemically stable in both a reducing and oxidizing atmosphere; (ii) they must have high electronic conductivity; and (iii) these thermal expansion coefficients must match those of other components in the cells. In addition, separator materials must be dense to prevent gas migration [1]. Because a cheap ferritic stainless-steel (Fe–Cr alloy) meets these requirements, it has been used to replace the lanthanum chromite-based ceramic as the technology of intermediate-temperature SOFCs (IT-SOFCs) that operate between 650 and 800 °C has progressed [3,4].

Ferritic stainless-steel is not only inexpensive but also has good physical and mechanical properties. On the other hand, the stainless-steel suffers from poor oxidation resistance. Oxidation causes the formation of a Cr_2O_3 scale. According to Samsonov [5], the Cr_2O_3 scale has a high specific electrical resistance, viz., $1 \times 10^2\ \Omega$ cm at 800 °C. Therefore, it can give rise to an increase in the resistance of an SOFC stack and to cause the Cr-poisoning at the interface between the perovskite-type cathode and the yttria-stabilized zirconia (YSZ) electrolyte.

Yenmiei et al. [6] have proposed the use of a perovskite coating of $LaCrO_3$ on the metallic interconnector material as an oxidation-protective layer. Although the lanthanum chromite phase has high electronic conductivity and good stability in both oxidizing and reducing atmospheres, it is difficult to synthesize

* Corresponding author. Tel.: +82 32 860 7521; fax: +82 32 862 4482.
E-mail address: hjhwang@inha.ac.kr (H.J. Hwang).

0378-7753/$ – see front matter © 2006 Elsevier B.V. All rights reserved.
doi:10.1016/j.jpowsour.2005.12.030

the chromite-based perovskite due to appreciable volatilization loss of chromium oxide at high sintering temperatures in an oxidizing atmosphere [7]. Different methods have been investigated for the production of protective coatings, e.g., plasma spray coating [8], electron-beam physical vapour deposition (EB-PVD) [9], and RF-magnetron sputtering [10]. These methods have some problems. For instance, plasma spray coating and physical vapor deposition require expensive vacuum equipment and the film deposition area is limited.

In this work, a lanthanum chromite-based perovskite is used as a coating material on a ferritic stainless-steel substrate, Fe–16Cr (SUS444) because it isolates the separator from reaction with the cathode material, has sufficient electric conductivity, and protects the substrate from oxidation. The perovskite structure has the general formula ABO_3, where the A-site cations are typically rare earth metals such as La, Pr, and Nd, while the B-sites are occupied by transition metals. Because strontium doping raises the thermal expansion coefficient of lanthanum chromite, the thermal expansion coefficient of the perovskite (10.2×10^{-6}–11.1×10^{-6} cm cm^{-1} K) is similar to that of Fe–Cr alloy (11.5×10^{-6} cm cm^{-1} K) [1]. Therefore, this study attempts to fabricate dense calcium or strontium-doped lanthanum chromite ($(La_{0.8}Ca_{0.2})CrO_3$ (LCC) and $(La_{0.8}Sr_{0.2})CrO_3$ (LSC) thin film layers by a sol–gel route. The fabrication process and characterization of the thin film layers are reported.

2. Experimental procedure

A commercial stainless-steel, SUS444 plate with a chemical composition of Fe–18.59Cr–1.96Mo–0.26Si–0.24Mn was used as the substrate for the coating. The sheet was cut into rectangular pieces of about 19 mm × 23 mm × 1.5 mm and the surfaces were polished with a series of increasingly finer grit SiC papers (#400–2000) and finally diamond paste (1–6 μm) to obtain a mirror surface. The polished substrates were ultrasonically cleaned in acetone for 20 min, rinsed in distilled water, soaked for 30 s in acetone, and dried with a nitrogen gas gun.

Precursor solutions for the perovskite thin film coating were prepared from starting materials of lanthanum(III) nitrate hexahydrate ($La(NO_3)_3{\cdot}6H_2O$, GFS Chemicals Inc., 99%), strontium nitrate ($Sr(NO_3)_2$, KANTO Chemical Co., 98%) or calcium nitrate tetrahydrate ($Ca(NO_3)_2{\cdot}4H_2O$, KANTO Chemical Co., 98%) and chromium(III) nitrate nonahydrate ($Cr(NO_3)_3{\cdot}9H_2O$ ACROS Organics, 99%). The preparation flow chart is shown in Fig. 1. The concentration of the precursor solution was 0.2 M and the atomic ratio of La, Sr or Ca, and Cr was 0.8:0.2:1. Appropriate quantities of the starting materials were dissolved in distilled water, then 40 ml ethylene glycol and 0.9 ml nitric acid were introduced. Heating and stirring of the solution on a hot plate at a controlled temperature of 80 °C for several hours resulted in a spinable precursor solution for coating.

$(La_{0.8}Sr_{0.2})CrO_3$ (LSC) and $(La_{0.8}Ca_{0.2})CrO_3$ (LCC) thin films were coated on the SUS444 substrate by a dip-coating technique. The speed at which the substrate was withdrawn from the precursor solution was 6 cm min^{-1}. The thickness of the deposited film on the substrate could be controlled by varying

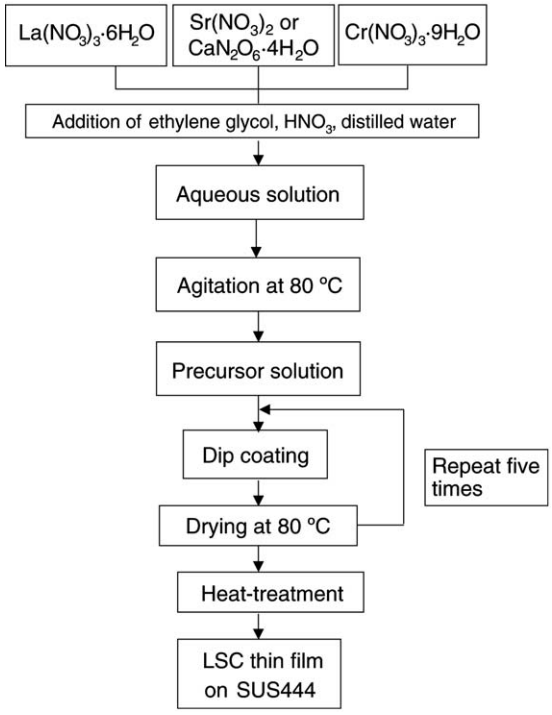

Fig. 1. Flow chart of experimental procedure.

the withdrawal speed and viscosity of the precursor solution. The viscosity of the precursor solutions for coating was 16 cP and slowly increased as the reaction time was prolonged. The viscosity of the coating solution was 23 cP.

The LSC- and LCC-coated substrates were dried on a hot plate at 80 °C to form gel films. The latter were then heat-treated at 300 °C for 10 min. The coating and drying process was repeated three to five times. The resulting thin films were finally heat-treated at various prescribed temperatures (400–800 °C) for 1 h. Both the dip-coated gel film and the heat-treated LSC and LCC films were transparent and had a uniform appearance with no cracks. In addition, there were no delamination or peel-off phenomena both in heat-treated samples and those subjected to repeated heat treatment at 800 °C.

The oxidation treatment was examined at 700 °C for 48 h in air. For comparison with non-coated SUS444, thin film-coated and non-coated substrates were oxidized simultaneously. In order to examine the extent of polymerization of the precursor solution as function of the reaction time, Fourier-transform infrared (FT-IR) spectra were recorded at a spectral resolution of 4 cm^{-1} (FT-IR, Bio-Rad, FTS-165). Crystallization and oxidation behaviour were investigated with a powder X-ray diffractometer (Philips, X'pert MPD) using Ni-filtered Cu K_α radiation. The surface and cross-sectional morphology of the coated samples were observed by scanning electron microscopy (SEM, HITACH, S-4200).

3. Results and discussion

The polymeric reaction was progressed in the precursor solution as a function of reaction time. The extent of polymerization was confirmed by FT-IR spectra and reflected the changes in the

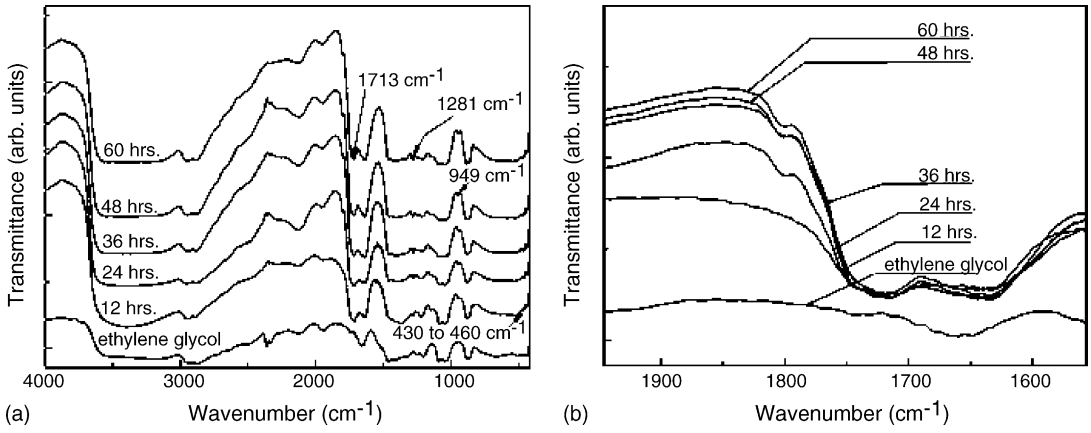

Fig. 2. (a) FT-IR spectra of ethylene glycol and LSC solutions in range 4000–400 cm^{-1}. The standing times are 6, 12, 18 and 24 h and (b) these spectra are shown in high magnification for the range 1946–1556 cm^{-1}.

molecular structure of the starting materials such as ethylene glycol and showed a chelating between cations and polymeric species. The polymeric reaction mechanism can be explained as follows [11,12]. The nitric acid, a powerful oxidizing agent, oxidizes the ethylene glycol in the precursor solution. The oxidized ethylene glycol is changed into oxalic acid. Then the esterification reaction commences between oxalic acid and the remaining ethylene glycol. The polyester allows homogeneous chelation of metal ions.

FT-IR transmission spectra of pure ethylene glycol and LSC precursor solutions are shown in Fig. 2(a). Pure ethylene glycol was used as a baseline for comparison purposes. The solutions for FT-IR analysis were prepared by heat-treating the precursor solutions at 80 °C for 12–60 h. The spectra contain the characteristic bands for C=O strong absorption ($\nu = 1713\ cm^{-1}$) after 24 h of reaction time [13,14]. Higher magnification of these spectra in the range 1946–1556 cm^{-1} is presented in Fig. 2(b). The absorption intensity of the bands of C=O groups gradually increase with reaction time at 80 °C, which means that ethylene glycol is converted to oxalic acid. The FT-IR spectra also show absorption bands at 1281 cm^{-1} due to the stretching mode of the O–C=O groups after 24 h of reaction. A new absorption band at 949 cm^{-1} was observed for LSC precursor solutions when compared with pure ethylene glycol. This absorption band indicates the presence of oxalate ions. It is considered that the weak absorption bands between 430 and 460 cm^{-1} indicate metal–oxygen bonds in the structure. From these results it can be inferred that ethylene glycol is oxidized by nitric acid to form polyesters.

X-ray diffraction patterns of LCC and LSC thin films coated on the SUS444 substrate are given in Fig. 3(a) and (b). The X-ray diffraction spectra, taken from the thin films, which were dip-coated on to the SUS444 substrate and subsequently heat-treated at 400–800 °C for 1 h, reveal that the thin films are $CaCrO_4$ (LCC) or $SrCrO_4$ (LSC) at the temperatures below 600 °C, and that the perovskite $LaCrO_3$ phase appears at temperatures above than 700 °C. Duran et al. [15] have described that a well-crystallized lanthanum chromate, $LaCrO_4$ is formed as a transient phase at temperatures below than 700 °C before formation of lanthanum chromite, $LaCrO_3$. In this study, however, the $LaCrO_4$ phase could not be detected in either LCC or LSC thin films on the SUS444 substrate. This is probably due to the strong interaction between the thin film and stainless-steel substrate. During the heat-treatment of the thin film, the stainless-steel (SUS444) can partially diffuse to react with the

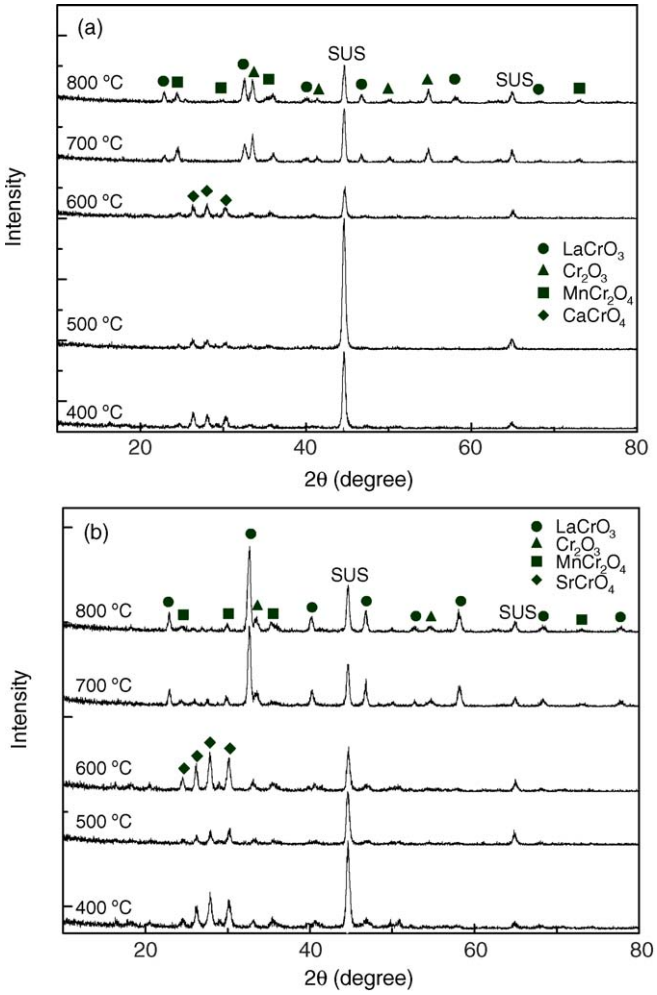

Fig. 3. XRD patterns of (a) LCC- and (b) LSC-coated SUS444 substrates heat-treated at 400–800 °C for 1 h.

LCC or LSC thin film. Thus, the phase evolution of the LCC and LSC thin films may be modified.

The relative intensity of the perovskite phase is increased with increasing heat-treatment temperature. At 800 °C, the thin films are composed of $LaCrO_3$, $MnCr_2O_4$ and Cr_2O_3. $MnCr_2O_4$ formation indicates the diffusion of manganese from the stainless-steel substrate, as reported by other researchers [16]. Generally, it is known that the $(Mn,Cr)_3O_4$ spinel phase is a semiconductor and shows relatively low electrical resistance [17]. The presence of the spinel phase is favourable for the operation of the metallic separator if the spinel layer remains fixed to the stainless-steel substrate under cyclic heat-treatment conditions. In addition, the $(Mn,Cr)_3O_4$ spinel phase is effective in reducing Cr-poisoning at the interfaces between the perovskite cathode and the YSZ electrolyte [10,18].

In the case of the LSC thin film, a large amount of $SrCrO_4$ phase is formed and it remains at 800 °C. By contrast, the relative intensity of the $SrCrO_4$ phase is decreased in the LCC thin films, as can be seen in Fig. 3(a). The $MCrO_4$ (M=Ca or Sr) phase obstructs sintering of alkaline earth metal-doped $LaCrO_3$ ceramics since its thermal expansion coefficient is much larger than that of $LaCrO_3$ [16]. According to Duran et al. [15], strontium in the perovskite structure is extruded to form the $SrCrO_4$. In order to clarify the formation of the $SrCrO_4$, ICP analysis on the precursor solution was performed. Although the target composition of the LCC and LSC thin films was $La_{0.8}Ca_{0.2}CrO_3$ and $La_{0.8}Sr_{0.2}CrO_3$, respectively, the atomic ratio of La, Ca (or Sr) and Cr of the precursor solution after reacting at 80 °C for 24 h was estimated to be 0.77:0.19:1 for both the LCC and LSC thin films. This result suggests that the excess Ca or Sr and Cr can react together to produce the $SrCrO_4$ phase at intermediate temperatures.

The surface microstructures of the LCC and LSC thin films on the SUS444 substrate after sintering at 700 °C for 1 h are shown in Fig. 4(a) and (b), respectively. Comparison of Fig. 4(a) and (b) shows that the LCC thin film has a dense microstructure. On the other hand, the microstructure of the LSC thin film is relatively porous. According to analysis performed by Mori et al. [19], the $SrCrO_4$ phase decomposes to $SrCrO_3$ and oxygen or $Sr(CrO_2)_2$ and oxygen; the oxgen may leave via pores in the microstructure [19]. From the XRD analysis shown in Fig. 3(b), it is found that large amount of $SrCrO_4$ are formed in the LSC thin film heat-treated at 600 °C. Although the $SrCrO_4$ phase disappears with increasing heat-treatment temperature, formation of the $SrCrO_4$ phase at the intermediate temperatures may be responsible for the porous microstructure of the LSC thin film.

The cross-section of the LSC thin film on the SUS444 substrate is shown in Fig. 5. The LSC thin film is well-adhered to the substrate. The thickness of the thin film layer is estimated to be approximately 1 μm, which is apparent from the SEM images in Fig. 5. The coating layer is continuous and fairly uniform in thickness. Although not shown in this study, it appears that a different substrate might result in a different microstructure and film thickness, even when the precursor solution and coating processes are completely the same.

The XRD patterns of the LCC- and LSC-coated and non-coated SUS444 substrates are presented in Fig. 6. The samples

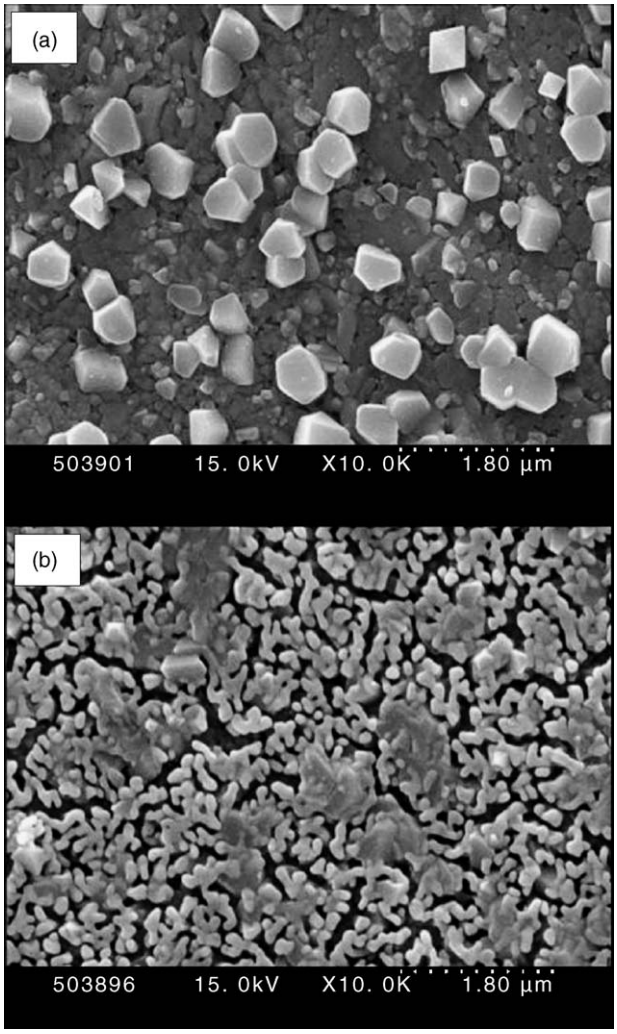

Fig. 4. Scanning electron micrographs of (a) LCC and (b) LSC thin films on SUS444 substrate (heat-treatment temperature at 700 °C).

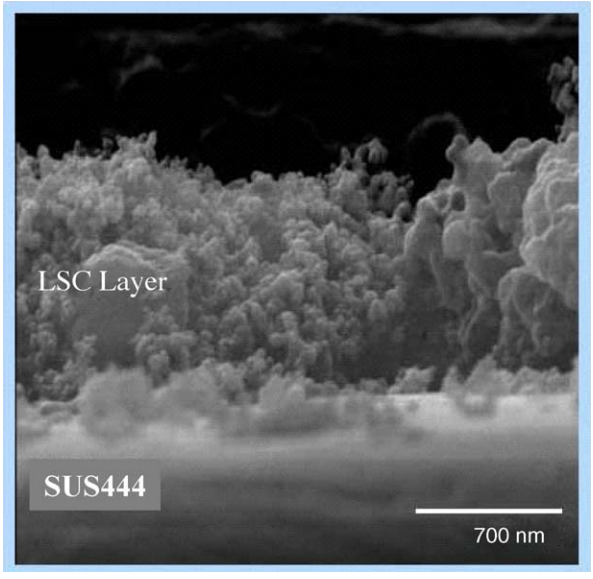

Fig. 5. Cross-section scanning electron micrographs of an LSC thin film coated on SUS444 substrate (heat-treated at 700 °C for 1 h).

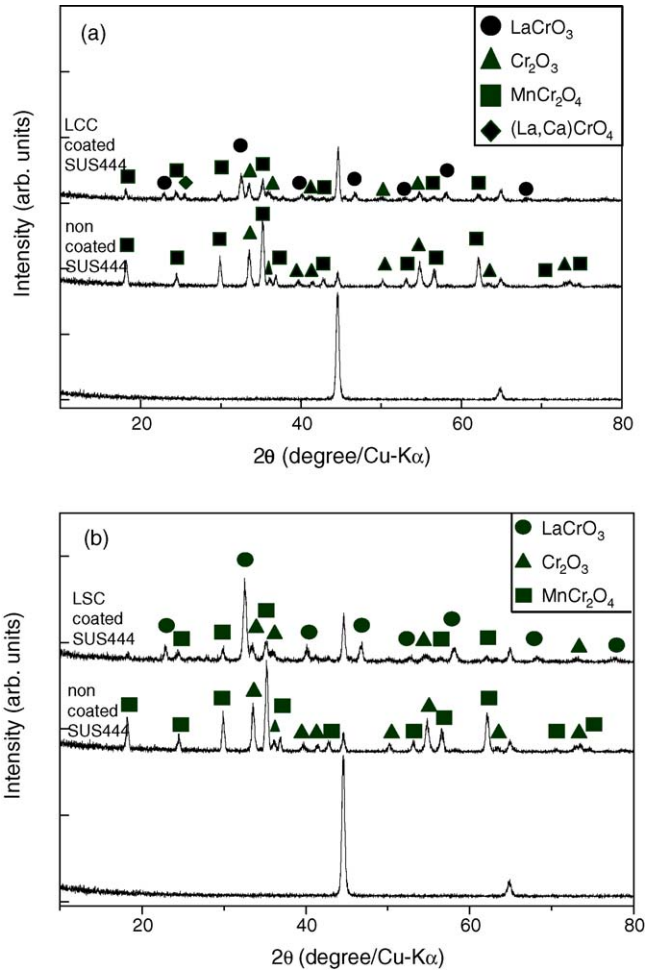

Fig. 6. XRD patterns of (a) LCC- and (b) LSC-coated SUS444 substrates heat-treated at 400–800 °C for 1 h in air.

were oxidized at 700 °C for 48 h in air. The LCC and the LSC-coated SUS444 substrates consist of $LaCrO_3$, Mn–Cr spinel and Cr_2O_3 phases, while the non-coated SUS444 substrate consisted of Cr_2O_3 and Mn–Cr spinel phases. Although the XRD patterns of the LCC- and LSC-coated SUS444 substrates indicate the presence of Mn–Cr spinel and Cr_2O_3, the relative intensities of the spinel and Cr_2O_3 phases are much weaker than those for the non-coated SUS444 substrate. In conclusion, the LCC and the LSC coating layers on the SUS444 substrate are effective in preventing oxidation at high temperature. Comparison of Fig. 6(b) with Fig. 6(a) shows that the relative intensities of the Cr_2O_3 phase in the LSC-coated SUS444 is much smaller than those for the LCC thin film-coated SUS444. This suggests that the LSC thin film-coated SUS444 is more resistant to oxidation than the LCC thin film-coated counterpart although the surface microstructure is much more porous. Therefore, the oxidation behaviour of the stainless-steel with the perovskite-type conductive oxide-coating layer may be strongly associated with the thickness, the composition and the microstructure of the film.

4. Conclusions

Calcium- or strontium-doped lanthanum chromite thin film layers are successfully fabricated by a dipping technique from precursor solutions of La, Ca (or Sr), Cr nitrates, nitric acid, and ethylene glycol. Polymerization of ethylene glycol and the chelating of cations are confirmed from FT-IR spectra of the precursor solution after reacting at 80 °C for 24 h. The LCC and LSC thin films have a perovskite structure and are uniformly deposited on the SUS444 substrate. A denser microstructure is observed for the LCC thin film on the substrate. The porous microstructure of the LSC thin film is considered to be attributed to the formation of the $SrCrO_4$ phase. It appears that the presence of both the LCC and LSC thin films effectively depresses oxidation of the SUS444 substrate. From a microstructural point of view, it is expected that the LCC thin film-coated substrate will exhibit better oxidation performance, but the result is found to be reverse. Thus, various factors that affect the oxidation behaviour of the substrate should be considered further.

Acknowledgements

The work was supported by the Core Technology Development Program for Fuel Cells of the Ministry of Science and Technology and the Korea Institute of Science and Technology Evaluation and Planning.

References

[1] N.Q. Minh, T. Takahash, Science and Technology of Ceramic Fuel Cell, first ed., Elsevier Science, Amsterdam, 1995, pp. 1–40.
[2] K. Eguchi, H. Kojo, T. Takeguchi, R. Kikuchi, K. Sasaki, Solid State Ionics 152,153 (2002) 411.
[3] T. Kadowaki, T. Shiomitsu, E. Matsuda, H. Nakagawa, H. Tsuneizumi, T. Maruyama, Solid State Ionics 67 (1993) 65.
[4] T. Brylewski, M. Nanko, T. Maruyama, K. Przybylski, Solid State Ionics 143 (2001) 131.
[5] G.V. Samsonov, The oxide Handbook, second ed., IFI/Plenum Data Company, New York, 1982, p. 125.
[6] H. Yenmiei, H. Michibata, T. Namikawa, Y. Yamazaki, Denki kagaku 58 (1990) 555.
[7] L. Groupp, H.U. Anderson, J. Am. Ceram. Soc. 59 (1976) 449.
[8] W.J. Quadakkers, H. Greiner, M. Hänsel, A. Pattanaik, A.S. Khanna, W. Malléner, Solid State Ionics 91 (1996) 55.
[9] N. Oishi, T. Namikawa, Y. Yamazaki, Surf. Coat. Technol. 132 (2000) 58.
[10] C. Johnson, R. Gemmen, N. Orlovskaya, Composites Part B 35 (2004) 167.
[11] J. March, Advanced Organic Chemistry: Reactions, Mechanisms and Structure, second ed., McGraw-Hill, New York, USA, 1968, p. 238.
[12] R.T. Morrison, R.N. Boyd, Organic Chemistry, sixth ed., Englewood, Prentice Hall, 1992, p. 725.
[13] R.M. Silverstein, G.C. Bassler, T.C. Morrill, Spectrometric Identification of Organic Compounds, fifth ed., John Wiley & Sons Inc., New York, USA, 1991, p. 104.
[14] C.J. Pouchert, The Aldrich Library of FT-IR Spectra Vapor Phase, first ed., Aldrich Chemical Company Inc., Wisconsin, 1985, p. 127, 490.
[15] P. Duran, J. Tartaj, F. Capel, C. Moure, J. Eur. Ceram. Soc. 24 (2004) 2619.
[16] H. Kurokawa, K. Kawamura, T. Maruyama, Solid State Ionics 168 (2004) 13.
[17] W.Z. Zhu, S.C. Deevi, Mater. Res. Bull. 38 (2003) 957.
[18] K. Fujita, T. Hashimoto, K. Ogasawara, H. Kameda, Y. Matsuzaki, T. Sakurai, J. Power Sources 131 (2004) 270.
[19] M. Mori, Y. Hiei, N.M. Sammes, Solid State Ionics 135 (2000) 743.